The tumor suppressor *CYLD* regulates entry into mitosis

Frank Stegmeier*, Mathew E. Sowa†, Grzegorz Nalepa†, Steven P. Gygi‡, J. Wade Harper†, and Stephen J. Elledge*§

*Department of Genetics, Harvard Medical School, Center for Genetics and Genomics, Howard Hughes Medical Institute, Brigham and Women's Hospital, Boston, MA 02115; and Departments of †Pathology and ‡Cell Biology, Harvard Medical School, Boston, MA 02115

Contributed by Stephen J. Elledge, April 9, 2007 (sent for review March 25, 2007)

Mutations in the cylindromatosis (*CYLD*) gene cause benign tumors of skin appendages, referred to as cylindromas. The *CYLD* gene encodes a deubiquitinating enzyme that removes Lys-63-linked ubiquitin chains from IκB kinase signaling components and thereby inhibits NF-κB pathway activation. The dysregulation of NF-κB activity has been proposed to promote cell transformation in part by increasing apoptosis resistance, but it is not clear whether this is *CYLD*'s only or predominant tumor-suppressing function. Here, we show that *CYLD* is also required for timely entry into mitosis. Consistent with a cell-cycle regulatory function, *CYLD* localizes to microtubules in interphase and the midbody during telophase, and its protein levels decrease as cells exit from mitosis. We identified the protein kinase Plk1 as a potential target of *CYLD* in the regulation of mitotic entry, based on their physical interaction and similar loss-of-function and overexpression phenotypes. Our findings raise the possibility that, as with other genes regulating tumorigenesis, *CYLD* has not only tumor-suppressing (apoptosis regulation) but also tumor-promoting activities (enhancer of mitotic entry). We propose that this additional function of *CYLD* could provide an explanation for the benign nature of most cylindroma lesions.

cell cycle | mitotic entry | Plk1 | siRNA screen

Familial cylindromatosis is an autosomal dominant predisposition to multiple benign neoplasms of skin appendages (called cylindromas), predominantly in their neck, face, and scalp (1). Cylindroma lesions exhibit biallelic loss of the tumor suppressor *CYLD* (2), which encodes a deubiquitinating enzyme. The loss of CYLD function leads to inappropriate NF-κB and JNK pathway activation and may trigger cell transformation in part through increased resistance to apoptosis (3–7). Although the molecular mechanisms are not entirely clear, CYLD has been proposed to inhibit NF-κB signaling by removing Lys-63 (K63)-linked polyubiquitin chains on upstream signaling components including TNF receptor-associated factor 2 (TRAF2), TRAF6, and NF-κB essential modulator (NEMO) (3–5).

We recently identified CYLD in a short hairpin RNA screen for novel cell-cycle regulators in human cells (8), raising the possibility that CYLD might have functions outside of its canonical role in NF-κB pathway regulation. Cell-cycle progression must be properly timed to faithfully replicate and partition the genetic material to the progeny cells. The timing of cell-cycle transitions is regulated by complex signal transduction pathways and monitored by checkpoint controls that delay the transition into subsequent cell-cycle phases until prior steps have been completed (9, 10). After the completion of DNA replication, for example, a tip in the balance between phosphorylation (Wee1 kinase) and dephosphorylation activities favors the activation of cyclin B–CDK1 (11, 12). The rapid increase in cyclin B–Cdk1 activity is reinforced by positive feedback loops involving the polo-like kinase Plk1 and phosphatases of the CDC25 family, thereby triggering the cell's entry into mitosis (13–15). The timing of mitotic entry is controlled by several surveillance pathways, most prominently the DNA damage and DNA replication checkpoints that delay mitotic entry in the presence of unreplicated or damaged DNA (16, 17). A less well characterized pathway, the prophase checkpoint (also referred to as antephase checkpoint), delays mitotic entry in response to impaired microtubule function (18). The only gene hitherto implicated in this checkpoint is *CHFR* (checkpoint with FHA and RING domains), which encodes an ubiquitin ligase, whose function and cell-cycle targets remain poorly understood (18–20).

In this study, we show that the deubiquitinating enzyme CYLD is required for timely entry into mitosis. We provide a detailed characterization of its cell-cycle regulatory function and discuss potential implications for CYLD's role in tumorigenesis.

Results

CYLD Regulates Premitotic Cell-Cycle Progression Independent of NF-κB Pathway Regulation. We recently identified *CYLD* in a short hairpin RNA screen that was designed to identify genes whose down-regulation results in delayed mitotic entry or defective spindle checkpoint function (8). The screen scored for reduced mitotic arrest in response to treatment with the spindle poison taxol. Importantly, three additional siRNAs targeting independent sequences within CYLD led to the accumulation of nonmitotic cells in the taxol assay, thereby validating the result from the primary short hairpin RNA screen (Fig. 1 *A* and *B*). Differences in nuclear morphology can be used to distinguish cells that delay/arrest before entering mitosis (normal interphase nuclear morphology) and checkpoint bypassing cells (multilobed nuclei) (8, 21). Based on that criterion, the normal interphase nuclear morphology of CYLD-depleted cells after taxol treatment (Fig. 1*C*) suggested that cells with reduced CYLD function delay cell-cycle progression before mitosis, which was further supported by FACS analysis [supporting information (SI) Fig. 6 *A* and *B*].

We next examined whether CYLD's deubiquitinating activity is required for its cell-cycle function. The premitotic "arrest" phenotype after CYLD depletion (using a siRNA targeting the 3′UTR) was significantly rescued after expression of a wild-type CYLD construct that lacks the 3′ UTR (Fig. 1*D*, CYLD-WT). In contrast, a catalytically inactive CYLD mutant (C601A; ref. 3) failed to restore the mitotic arrest (Fig. 1*D*, CYLD-ci), demonstrating that CYLD's deubiquitinating activity is required for its cell-cycle function. Because CYLD has been shown to negatively regulate IκB kinase (IKK)/NF-κB signaling, it is possible that CYLD regulates cell-cycle progression indirectly by

Author contributions: F.S., M.E.S., J.W.H., and S.J.E. designed research; F.S., M.E.S., G.N., and S.P.G. performed research; S.P.G. contributed new reagents/analytic tools; F.S., M.E.S., J.W.H., and S.J.E. analyzed data; and F.S., J.W.H., and S.J.E. wrote the paper.

The authors declare no conflict of interest.

Freely available online through the PNAS open access option.

Abbreviations: IKK, IκB kinase; CHFR, checkpoint with FHA and RING domains; K63-ub, Lys-63-linked ubiquitin; NEMO, NF-κB essential modulator; P-H3, phosphohistone H3; HGS, hepatocyte growth factor-regulated tyrosine kinase substrate.

§To whom correspondence should be addressed. E-mail: selledge@genetics.med.harvard.edu.

This article contains supporting information online at www.pnas.org/cgi/content/full/0703268104/DC1.

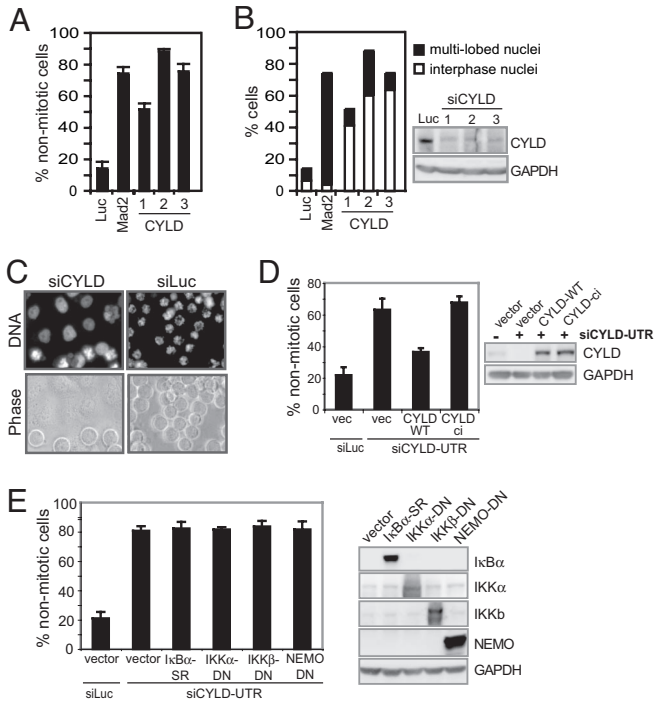

Fig. 1. CYLD regulates premitotic cell-cycle progression independent of NF-κB pathway regulation. (*A* and *B*) HeLa cells were transfected with siRNAs (numbers refer to different oligos), treated with 100 nM Taxol 48 h posttransfection, and fixed for visual inspection 24 h after taxol addition. The percentage of nonmitotic cells (*A*) and cells with multilobed or interphase nuclei (*B*) was quantified. Mad2 siRNAs were used as a positive control for a spindle checkpoint regulator. The values represent averages of three independent experiments ($n = 100$, error bars ± 1 SD). The Western blot in *B* shows the extent of CYLD protein depletion 48 h after siRNA transfection. (*C*) Representative images of HeLa cells transfected with siRNAs targeting luciferase (control) or CYLD (oligo1) that illustrate the premitotic nuclear morphology of CYLD-depleted cells. (Magnification: ×20.) (*D*) Transfection of siRNA-resistant wild-type HA-tagged CYLD (CYLD-WT), but not the catalytically inactive-mutant (CYLD-ci), rescues the premitotic delay of CYLD siRNA-treated cells. HeLa cells were transfected with the indicated siRNAs (CYLD siRNA targets the 3′ UTR). After 24 h, the rescuing plasmids were cotransfected with H2B-GFP. Forty-eight hours after siRNA transfection, 100 nM taxol was added for an additional 24 h before fixation. GFP-positive cells were analyzed for the percentage of nonmitotic cells ($n = 100$, error bars ± 1 SD). The Western blot shows similar expression levels of wild-type and mutant HA-CYLD. (*E*) Down-regulation of NF-κB signaling does not rescue CYLD's cell-cycle defect. HeLa cells were transfected with the indicated siRNAs. Twenty-four hours later, the indicated NF-κB inhibitory plasmids were cotransfected with H2B-GFP. GFP-positive cells were analyzed for the percentage of nonmitotic cells ($n = 100$, error bars ± 1 SD). The Western blot shows expression of NF-κB inhibitory constructs.

increasing NF-κB pathway activity. We therefore examined the effects of inhibiting this signaling cascade at multiple steps by using dominant negative constructs. Although all of the tested constructs were able to inhibit NF-κB translocation in response to TNF-α signaling (SI Fig. 6*C*), none reversed the cell-cycle defects caused by CYLD down-regulation (Fig. 1*E*). In addition, the extent of IκBα phosphorylation (the substrate of the IKK complex) was similar in control and CYLD-depleted cells (data not shown), consistent with CYLD regulating NFκB signaling after stimulation but not its basal activity (4, 6). Together, these findings suggest that CYLD's deubiquitination activity regulates cell-cycle progression independent of its canonical role in NF-κB pathway regulation.

CYLD Is Required for Efficient Entry into Mitosis. The premitotic arrest phenotype in cells with reduced CYLD function could be caused by delayed progression through the G_1, S, or G_2 phases of the cell cycle. To distinguish between theses possibilities, we synchronously released CYLD-depleted cells from a mitotic arrest and monitored progression through subsequent cell-cycle stages. CYLD-depleted cells exhibited a minor delay in the G_1–S transition but progressed normally through S phase (SI Fig. 7). In contrast, cells with reduced CYLD function were markedly impaired in mitotic entry, as judged by the delayed accumulation of the mitotic marker phospho-histone H3 (P-H3) compared with control-treated cells (Fig. 2*A*). The phosphorylation of Cdc25C, a positive regulator of mitotic entry (22, 23), was also delayed after CYLD down-regulation (Fig. 2*A*). Impaired Cdc25C phosphorylation has previously been observed in cells with reduced Plk1 function (14, 24, 25). We therefore directly compared the mitotic entry defect of cells with decreased expression of Plk1 or CYLD. Notably, cells depleted for CYLD or Plk1 delayed mitotic entry and Cdc25C phosphorylation to a similar extent (Fig. 2 *B–D*). Moreover, the degradation of Emi1, which requires a priming phosphorylation by Plk1 (26, 27), was equally delayed after CYLD or Plk1 down-regulation (Fig. 2*C*). We were able to exclude the possibility that the observed mitotic entry delay was caused by replication problems, because CYLD-depleted cells completed DNA replication with wild-type kinetics (Fig. 2*E*) and showed no evidence of DNA damage checkpoint activation (as monitored by Chk1 phosphorylation; SI Fig. 8). Together, these findings demonstrate that CYLD function is required for efficient mitotic entry.

In the synchronous release experiments, we noted that CYLD protein levels decreased as cells exited mitosis, remained low in G_1, and reaccumulated as cells entered S phase (Fig. 2 *A* and *C*). Moreover, CYLD protein stability rapidly decreased as cells exited from mitosis (Fig. 3). Other important cell-cycle regulators, such as Cyclin B or Plk1 (28), are degraded as cells exit from mitosis, thereby helping to reset the cell cycle from the mitotic to the G_1 state. Thus, the cell-cycle-dependent changes in protein levels are consistent with CYLD having an important cell-cycle regulatory function.

CYLD Localizes to the Midbody and Its Overexpression Leads to Multinucleated Cells. We generated tetracycline-inducible cell lines to assess the effect of CYLD overexpression. Notably, elevated levels of wild-type CYLD led to a strong increase in fragmented nuclei and multinucleated cells (Fig. 4 *A–C*, TET-CYLD-WT). This phenotype depended on CYLD's catalytic activity because it was not observed when we overexpressed the catalytically inactive mutant (Fig. 4 *A–C*, TET-CYLD-ci). The accumulation of multinucleated and fragmented nuclei is most likely a result of impaired mitotic progression and/or cytokinesis defects.

Many critical regulators of cytokinesis, such as the chromosomal passenger complex and Plk1, localize to the central spindle and midbody during telophase (29, 30). CYLD contains three CAP–GLY domains, which are found in several microtubule-interacting proteins (31). When we examined the subcellular localization of ectopically expressed CYLD fused to GFP, we found that CYLD–GFP colocalized with the microtubule cytoskeleton in interphase cells (Fig. 4*D*). Strikingly, CYLD staining was enriched at the midbody during telophase (Fig. 4 *D* and *E*). This finding further substantiates the idea that CYLD may directly regulate cytokinesis.

CYLD Associates with Plk1. To gain insight into how CYLD may regulate cell-cycle progression, we used a proteomic approach to search for potential CYLD substrates. We immunopurified stably expressed N-terminal HA-Flag-tagged CYLD and identified copurifying proteins by mass spectrometry (Fig. 5*A*). Because most enzyme–substrate interactions are likely to be transient, a chemical cross-linking reagent was added with the

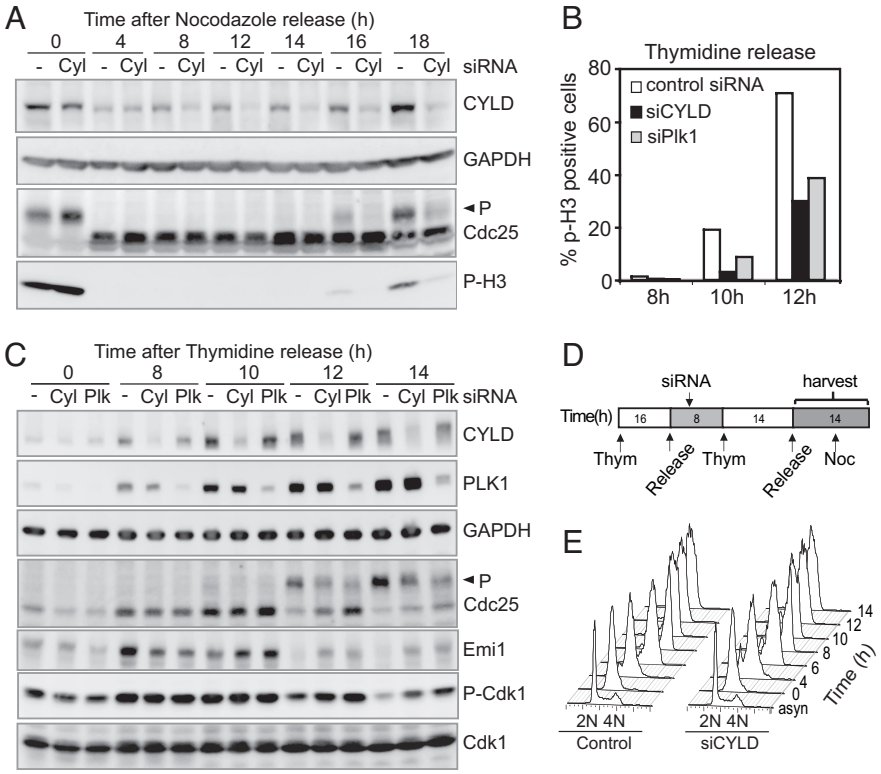

Fig. 2. CYLD is required for timely entry into mitosis. (*A*) HeLa cells were treated with siRNAs targeting luciferase (−) or CYLD (Cyl), synchronized in mitosis (100 ng/ml nocodazole), and released into fresh medium, and nocodazole was readded 6 h after release to arrest cells in the next mitosis. For detailed synchronization protocol see SI Fig. 6*D*. Cell extracts were collected at the indicated time points and immunoblotted for CYLD, GAPDH, Cdc25C (arrowhead indicates phosphorylation form), and P-H3 (serves as mitotic marker). (*B–D*) HeLa cells were treated with the indicated siRNAs, synchronized at the G_1/S transition by a double thymidine block, and released from the second thymidine block into medium containing 100 ng/ml Nocodazole (added 6 h after release) to arrest cells in mitosis. (*B*) FACS sorting for P-H3-positive cells was used to determine the percentage of mitotic cells at the indicated time points. (*C*) Cell extracts were collected and immunoblotted for the indicated proteins (P-Cdk1, antibody recognizing Y15-phosphorylated Cdk1). (*D*) Schematic of synchronization protocol applied in *B–E*. (*E*) FACS profiles (DNA staining) of control and CYLD-depleted cells showing that DNA replication occurs with normal kinetics in cells with reduced CYLD function.

goal of stabilizing such transient and weak interactions. After processing the list of identified proteins and subtraction of proteins found in the control purification, we searched this final list of 81 proteins for those implicated in G_2/M progression and identified Plk1 (Fig. 5*B* and SI Table 1). This was particularly intriguing because Plk1 and CYLD exhibit similar loss-of function (mitotic entry defects; Fig. 2*C*) and overexpression phenotypes (Fig. 4*B* and ref. 32), raising the possibility that CYLD and Plk1 might function together within the same signaling pathway. Immunoprecipitation experiments confirmed that CYLD interacts with Plk1 but not other cell-cycle regulators such as Cyclin B or Securin when expressed ectopically or at endogenous levels (Fig. 5 *C* and *D*). Together, these findings are consistent with the idea that CYLD may regulate mitotic entry and/or cytokinesis together with Plk1, possibly by modulating Plk1 activity (see *Discussion*).

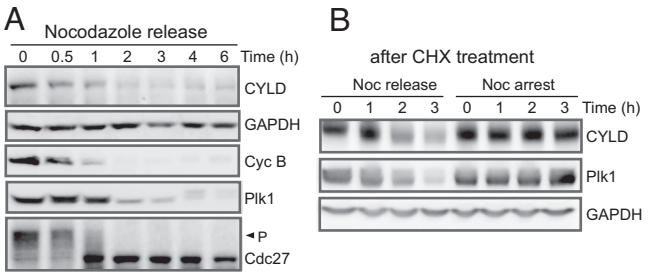

Fig. 3. CYLD is degraded as cells exit from mitosis. (*A*) HeLa cells were released from a mitotic arrest (100 ng/ml Nocodazole), and cell lysates were blotted with the indicated antibodies. The faster migration of Cdc27 (1 h time point) indicates dephosphorylation and serves as a marker for exit from mitosis. (*B*) HeLa cells were synchronized in mitosis (100 ng/ml Nocodazole, Noc), 10 mM Cycloheximide (CHX) was added (to prevent *de novo* protein synthesis), and Nocodazole was either released from (Noc release) or cultured in the continued presence of nocodazole (Noc arrest). Cell lysates were analyzed by Western blotting.

Discussion

Familial cylindromatosis patients generally inherit one defective *CYLD* allele (often a point mutant or frame shift) and exhibit loss of heterozygosity for the remaining wild-type allele in the developing skin lesions, providing strong evidence for *CYLD*'s function as a tumor suppressor gene (2). Recent studies proposed that loss of CYLD promotes tumor progression at least in part by hyperactivating the antiapoptotic signaling of the NF-κB and JNK pathways (3–7).

In this study we show that CYLD also regulates entry into mitosis. Notably, this cell-cycle function of CYLD appears to be independent of its canonical role in IKK/NF-κB signaling. Consistent with its cell-cycle function, CYLD protein levels decrease as cells exit from mitosis, remain low during G_1, and reaccumulate during the subsequent S phase. The degradation of CYLD at the end of mitosis is characteristic of anaphase-promoting complex (APC) substrates such as Plk1 and Cyclin B. Although CYLD contains two perfect D-boxes and a KEN-box,

CELL BIOLOGY

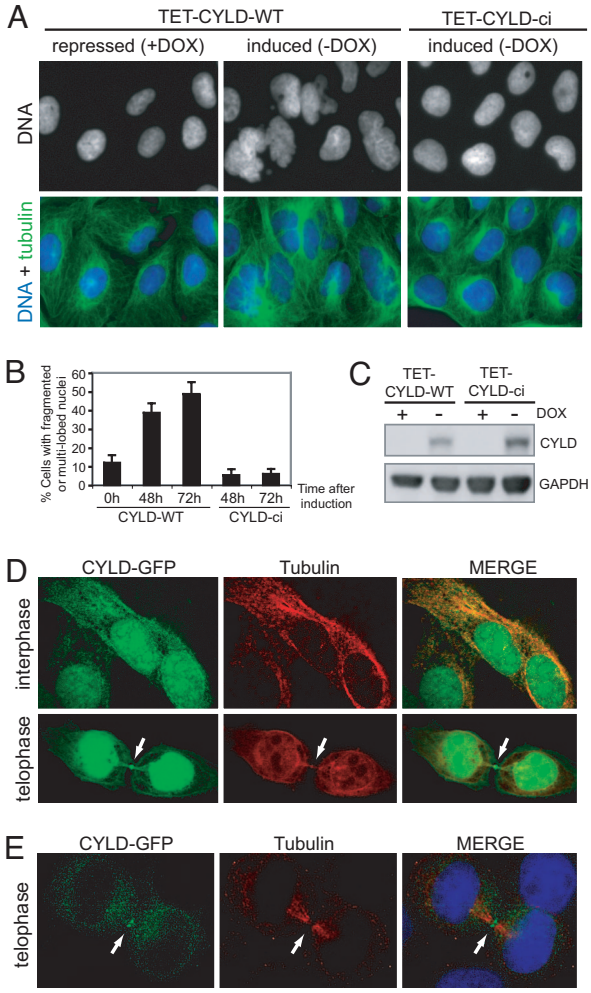

Fig. 4. CYLD overexpression leads to accumulation of multinucleated cells. (*A–C*) U2OS TET-OFF cells stably expressing tetracycline-responsive wild-type (TET-CYLD-WT) or catalytically inactive CYLD mutant (TET-CYLD-ci) were either cultured in the presence (+DOX, repressed) or absence (−DOX, induced) of doxycycline (DOX, tetracycline analog). (*A*) Representative images taken 48 h after doxycycline treatment illustrate the presence of multinucleated nuclei after CYLD overexpression. (*B*) The percentage of cells with fragmented or multilobed nuclei was quantified ($n > 100$, error bars $\pm$ 1 SD). (*C*) A Western blot showing expression levels of wild-type and mutant CYLD. (*D* and *E*) CYLD localizes to the microtubule cytoskeleton in interphase and is enriched at the midbody (marked by arrow) during telophase. (*D*) HeLa cells were transiently transfected with GFP–CYLD and its localization was assessed by indirect immunofluorescence. Tubulin is stained in red. (*E*) HeLa cells stably expressing low levels of GFP-CYLD (green) were probed for tubulin (red) and stained for DNA (blue). (Magnifications: ×100.)

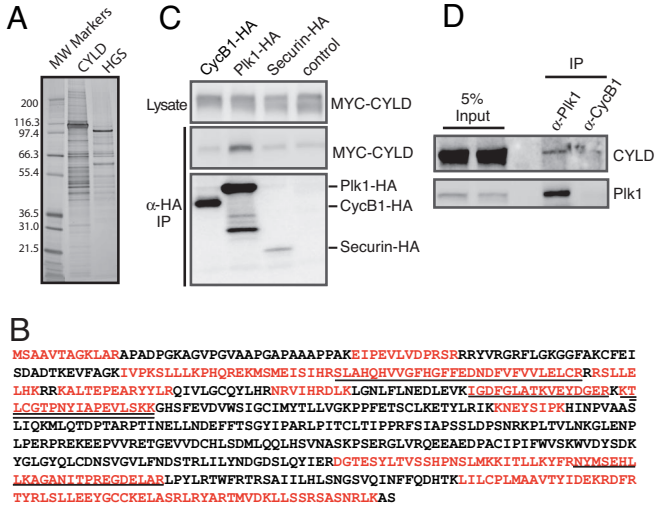

Fig. 5. CYLD associates with Plk1 *in vivo*. (*A*) α-HA purification of stably integrated retrovirally expressed HA-Flag-CYLD from 293T cells shows that CYLD copurifies with multiple proteins not found in control purifications (HGS; see *Materials and Methods*). Ten percent of each HA peptide elution was analyzed by SDS/PAGE using a 4–12% gradient gel and silver stained. (*B*) Mass spectrometry analysis of purified CYLD-interacting proteins identifies Plk1. Total peptides identified in raw mass spectrometry data (with no filtering) are shown in red, and the five peptides found after stringent filtering (see *Materials and Methods*) are underlined. (*C*) Exogenously expressed CYLD associates with Plk1. HeLa cells were transiently transfected with the indicated MYC-tagged expression constructs and HA-Plk1. Anti-HA immunoprecipitates (IP) were probed with α-MYC (*Upper*) and α-HA antibodies (*Lower*). (D) Endogenous CYLD associates with Plk1. Plk1 was immunoprecipitated (IP) with α-Plk1 or α-CycB1 (control) antibodies, and the immunoprecipitates were probed for CYLD and Plk1.

which are known to target substrates to the APC, we were unable to detect CYLD ubiquitination or degradation by using *in vitro* APC assays (data not shown), implying that another ubiquitin ligase might be responsible for its cell-cycle-regulated proteolysis. Further studies will be needed to determine whether CYLD is also cell-cycle-regulated at the level of transcription and whether this contributes to fluctuation of protein levels. We would like to note that the cell-cycle-dependent fluctuations of CYLD protein levels might have implications for IKK/NF-κB signaling, raising the possibility that cells are most responsive to IKK-stimulatory signals (such as TNF-α) during G_1, when the levels of CYLD are lower than during other cell-cycle stages.

Ubiquitin-mediated proteolysis, which is mediated by Lys-48-linked polyubiquitin (K48-ub) chains that target substrates for proteasomal degradation, has been well established as a critical cell-cycle regulatory mechanism for over a decade (33). However, several recent studies point toward an important role of noncanoncial polyubiquitin chains, in particular Lys-63-linked ubiquitin (K63-ub) chains, in cell-cycle regulation. K63-ub chains are thought to regulate protein–protein interactions and modulate target protein activities rather than constituting a degradation signal (34). The prophase checkpoint protein CHFR, for example, encodes an ubiquitin ligase that catalyzes the formation of K63-ub chains (20). More recently, K63-linked polyubiquitination of the chromosomal passenger protein survivin has been proposed to regulate its dynamic kinetochore localization (35). Our study provides further evidence for the importance of K63-ub in cell-cycle progression, because the deubiquitinating enzyme CYLD, which has been shown to preferentially if not exclusively target K63-ub chains *in vivo* (3–5), is required for efficient mitotic entry.

How does CYLD regulate entry into mitosis? The finding that CYLD's deubiquitination activity, but not NF-κB signaling, is required for its cell-cycle function, suggests that CYLD deubiquitinates a regulator of mitotic entry. We provide several lines of evidence that CYLD and Plk1 function within the same pathway. First, the mitotic entry defects after CYLD or Plk1 downregulation are strikingly similar. In particular, the phosphorylation of Cdc25C, an established Plk1 target (14, 24, 25, 36) and the degradation of Emi1, which depends on prior phosphorylation by Plk1 (26, 27), are significantly delayed also in CYLD-depleted cells. Moreover, overexpression of CYLD phenocopies the multinucleation phenotype observed in cells with elevated Plk1 activity (32). Together, these findings suggest that CYLD functions either upstream of or in parallel to Plk1. Based on the physical *in vivo* interaction of CYLD and Plk1, we favor the

possibility that CYLD directly regulates the polyubiquitination levels of Plk1. The finding that reduced levels of CYLD did not affect Plk1 protein levels (Fig. 2*C*) argues that CYLD does not regulate Plk1 stability by modulating K48-ub chains. Because CYLD is thought to target K63-ub chains (3–5), CYLD may regulate Plk1 activity by deubiquitinating K63-ub chains on Plk1 or its upstream regulators. Given that CYLD and CHFR possess opposing enzymatic activities (both targeting K63-ub chains), it is tempting to speculate that CYLD may be required to restart the cell cycle after CHFR-mediated prophase arrest by deubiquitinating the targets of CHFR, possibly including Plk1, a proposed target of CHFR (19). In this model, CYLD may only be required for the initial activation of Plk1 at the G_2/M transition and no longer be required for Plk1 function at later cell-cycle stages, thereby explaining why both CYLD and Plk1 are required for efficient mitotic entry, but only Plk1 depletion leads to monopolar spindle formation and mitotic arrest.

What are the implications of our study for CYLD's role in tumorigenesis? Paradoxically, one would expect that CYLD's cell-cycle regulatory functions described here should promote tumor growth rather than being tumor suppressing. It is important to note that CYLD down-regulation delays but does not entirely block the G_2/M progression, thus causing only a subtle proliferative disadvantage. Furthermore, the dependency on CYLD function for efficient mitotic entry could differ between different tissue types and/or may be compensated by up-regulation of functionally redundant deubiquitinating enzymes after loss of CYLD function, possibly contributing to the striking tissue tropism of CYLD. Because most cylindroma lesions are of benign nature, an intriguing possibility is that the proliferative disadvantage caused by loss of CYLD function helps to restrain tumor growth and thus forestalls progression to malignancy. Alternatively, a defect in cell-cycle progression could contribute to tumorigenesis by promoting genomic instability. These possibilities will require further exploration to resolve.

Materials and Methods

Plasmids and siRNA Reagents. The coding sequences for CYLD were PCR-cloned into Gateway-compatible entry vectors and transferred into epitope-tagged (N terminus) expression vectors (gift from Jianping Jin, Harvard Medical School) by using a LR recombination kit (Invitrogen, Carlsbad, CA). The catalytic inactive CYLD (C601A, CYLD-ci) was constructed by site-directed mutagenesis using a QuikChange kit (Stratagene, La Jolla, CA). The IKKβ-ΔN (dominant negative), IKKα-ΔN, NEMO-ΔN, and IκBα-SR (superrepressor) were a gift from J. Li (University of Southern California, Los Angeles, CA) (37). The following siRNA oligonucleotides (Dharmacon, Lafayette, CO) were used in this study: CYLD-si1 (CGAAGAGGCTGAATCATAA), CYLD-si2 (CGCTGTAACTCTTTAGCAT), CYLD-si3 (GAACTCACATGGTCTAGAA), CYLD-siUTR (GCAGAGTCCTAACGTTGCA), and Plk1 (CGGCAGCGUGCAGAUCAAC). For control siRNA treatment, siRNAs targeting luciferase (CGTACGCGGAATACTTCGA) were used. CYLD-si2 was used for the synchronous release experiments in Fig. 2. Cells were transfected with siRNAs (100 nM) using Oligofectamine (Invitrogen) according to the manufacturer's protocol.

Cell Culture and Synchronization. HeLa cells were grown in DMEM supplemented with 10% FBS and antibiotics. Inducible CYLD-overexpression cell lines were generated by transfecting U2OS TET-OFF cell lines (gift from C. Lindon, Wellcome/Cancer Research Institute, Cambridge, U.K.) with pTRE$_{tight}$-FLAG-CYLD or pTRE$_{tight}$-FLAG-CYLD-ci(C601A), followed by the isolation of clonal cell lines. For the nocodazole release experiment, cells were treated for 24 h with thymidine (2.5 mM), released for 14 h into fresh medium containing nocodazole (100 ng/ml), and released from the mitotic arrest by washing three times with PBS and plating into fresh medium. To study the effects of CYLD and Plk1 down-regulation on cell-cycle progression, cells were treated with thymidine (2.5 mM) for 16 h. After releasing cells for 2 h, cells were transfected with siRNAs. Seven hours after release from the first thymidine block, thymidine was readded for an additional 17 h. Cells were released from the second thymidine block into medium containing 100 ng/ml Nocodazole to arrest cells in mitosis and prevent them from entering the next cell cycle (see schematic in Fig. 2*D*).

Flow Cytometry. Cells were harvested and fixed in ice-cold 70% ethanol. Cell-cycle distribution and P-H3 (Upstate Biotechnology, Lake Placid, NY) positivity were analyzed by using flow cytometry of 10,000 events (Cytomics FC 500; Beckman Coulter, Fullerton, CA).

Immunoblotting and Immunoprecipitation. Whole-cell extracts were prepared by cell lysis in SDS sample buffer, resolved by SDS/PAGE, transferred to nitrocellulose membranes, and probed with the indicated antibodies. Rabbit CYLD (gift from S. Sun, Pennsylvania State College of Medicine, Hershey, PA), rabbit anti-Cdc27 (sc-5618; Santa Cruz Biotechnology), mouse anti-Cyclin B1 (sc-245; Santa Cruz Biotechnology), rabbit anti-GAPDH (Santa Cruz Biotechnology), rabbit anti-Cdc25 (Santa Cruz Biotechnology), rabbit anti-P-H3 (Upstate Biotechnology), mouse anti-Plk1 (Santa Cruz Biotechnology), rabbit anti-Emi1 (gift from P. Jackson, Genentech, San Francisco, CA), rabbit anti-phospho-Cdk1 (Y15-P specific; Cell Signaling, Beverly, MA), and rabbit anti-Cdk1 (Santa Cruz Biotechnology). For immunoprecipitations, cells were lysed in CHAPS lysis buffer [50 mM Tris·HCl, pH 7.5/150 mM NaCl/0.3% CHAPS/EDTA-free complete protease inhibitor mix (Roche, Indianapolis, IN)]. Primary antibodies were added to cleared lysates for 2 h, followed by a 3-h rotation with protein G-Sepharose beads (Pierce, Rockford, IL) at 4°C. The beads were then washed five times with CHAPS lysis buffer. The proteins bound to the beads were dissolved in SDS sample buffer, separated by SDS/PAGE, and blotted with the indicated antibodies.

Immunofluorescence Microscopy. Cells were fixed, permeabilized, and blocked as described (21). For immunostaining, mouse antitubulin (Molecular Probes, Carlsbad, CA), anti-p65 (NF-κB, Santa Cruz Biotechnology), and cross-adsorbed secondary antibodies from molecular probes were used. DNA was stained with DAPI. A Deltavision (San Diego, CA) RT microscope equipped with a $\times$40 or $\times$100 objective was used for image acquisition.

HA Purification and Mass Spectrometry. CYLD was cloned into the MSCV N-terminal HA-Flag (NTAP) vector by using the Gateway LR reaction. Stable integrants were selected with puromycin at a final concentration of 1 μg/ml in DMEM plus 10% FBS. Expression of the transgene was confirmed by anti-HA Western blots (data not shown) of whole-cell lysate. Stable hepatocyte growth factor-regulated tyrosine kinase substrate (HGS) expressing 293T cells was generated in the same manner to use as a control for identifying CYLD-specific proteins. For the purification, cells were harvested in PBS and lysed in lysis buffer [50 mM Hepes, pH 7.5/150 mM NaCl/0.5% Nonidet P-40/protease inhibitor mixture (Roche)]. Cleared lysates were incubated with 0.25 μg/ml DTSSP [3,3′-dithiobis (sulfosuccinimidylpropionate), cross-linking reagent] for 30 min on ice and then quenched with 1/10 volume of 1 M Tris, pH 7.5. Protein complexes were purified by using α-HA agarose beads (Sigma, St. Louis, MO) with overnight incubation at 4°C, sequentially washed with lysis buffer, and eluted with 0.25 μg/ml HA peptide (Sigma) in a final volume of 100 μl. After elution, 50 mM DTT

was added to reverse the DTSSP cross-linking. Ten percent of the elution was analyzed by SDS/PAGE and silver stain, whereas the remaining sample was precipitated with trichloroacetic acid, digested with trypsin, and then analyzed with an LTQ LC/MS/MS mass spectrometer (Thermo Finnigan, San Jose, CA). MS/MS spectra were searched against a human tryptic peptide library by using a target-decoy database strategy and the Sequest algorithm. Initial protein matches from the CYLD purification were filtered to obtain ≈2% false positives, resulting in 222 identified proteins. The original MS/MS spectra were then searched against a database containing only those 222 proteins, and the results were filtered for peptides with XCorr values > 2.5 for 2+ charge state, 3.2 for 3+ charge state, and a DeltaCn score of >0.25. Protein matches with more than one peptide were selected to produce a final list of 131 proteins. The data for HGS were searched against the CYLD-specific database, filtered as described above, and then compared with the results obtained from the CYLD analysis. Interactors identified also in the control HGS purification, which are likely to represent nonspecific interactions, were removed from the CYLD interaction data set. The 81 proteins found only in the CYLD data are presented in SI Table 1.

We thank S. Sun, P. Jackson, C. Lindon, J. Li, and J. Jin for gifts of reagents and members of S.J.E.'s laboratory for helpful discussions. F.S. is a Fellow of the Helen Hay Whitney Foundation. M.E.S. is supported by a postdoctoral fellowship from the American Cancer Society. This work was supported by grants from the National Institutes of Health (to S.J.E. and W.H.) and the Department of Defense (to S.J.E.). S.J.E. is an Investigator of the Howard Hughes Medical Institute.

1. van Balkom ID, Hennekam RC (1994) *J Med Genet* 31:321–324.
2. Bignell GR, Warren W, Seal S, Takahashi M, Rapley E, Barfoot R, Green H, Brown C, Biggs PJ, Lakhani SR, *et al.* (2000) *Nat Genet* 25:160–165.
3. Brummelkamp TR, Nijman SM, Dirac AM, Bernards R (2003) *Nature* 424:797–801.
4. Kovalenko A, Chable-Bessia C, Cantarella G, Israel A, Wallach D, Courtois G (2003) *Nature* 424:801–805.
5. Trompouki E, Hatzivassiliou E, Tsichritzis T, Farmer H, Ashworth A, Mosialos G (2003) *Nature* 424:793–796.
6. Reiley W, Zhang M, Sun SC (2004) *J Biol Chem* 279:55161–55167.
7. Massoumi R, Chmielarska K, Hennecke K, Pfeifer A, Fassler R (2006) *Cell* 125:665–677.
8. Stegmeier F, Rape M, Draviam V, Nalepa G, Sowa M, McDonald R, Li M, Hannon G, Sorger P, Kirschner M, *et al.* (2007) *Nature* 446:876–891.
9. Murray AW (1995) *Curr Opin Genet Dev* 5:5–11.
10. Nasmyth K (1996) *Science* 274:1643–1645.
11. Takizawa CG, Morgan DO (2000) *Curr Opin Cell Biol* 12:658–665.
12. Coleman TR, Dunphy WG (1994) *Curr Opin Cell Biol* 6:877–882.
13. Abrieu A, Brassac T, Galas S, Fisher D, Labbe JC, Doree M (1998) *J Cell Sci* 111:1751–1757.
14. Qian YW, Erikson E, Taieb FE, Maller JL (2001) *Mol Biol Cell* 12:1791–1799.
15. Pomerening JR, Sontag ED, Ferrell JE, Jr (2003) *Nat Cell Biol* 5:346–351.
16. Nyberg KA, Michelson RJ, Putnam CW, Weinert TA (2002) *Annu Rev Genet* 36:617–656.
17. Kastan MB, Bartek J (2004) *Nature* 432:316–323.
18. Scolnick DM, Halazonetis TD (2000) *Nature* 406:430–435.
19. Kang D, Chen J, Wong J, Fang G (2002) *J Cell Biol* 156:249–259.
20. Bothos J, Summers MK, Venere M, Scolnick DM, Halazonetis TD (2003) *Oncogene* 22:7101–7107.
21. Draviam V, Stegmeier F, Nalepa G, Sowa M, Chen J, Liang A, Hannon G, Sorger P, Harper W, Elledge S (2007) *Nat Cell Biol*, 10.1038/ncb1569.
22. Kumagai A, Dunphy WG (1991) *Cell* 64:903–914.
23. Bulavin DV, Higashimoto Y, Demidenko ZN, Meek S, Graves P, Phillips C, Zhao H, Moody SA, Appella E, Piwnica-Worms H, Fornace AJ, Jr (2003) *Nat Cell Biol* 5:545–551.
24. Qian YW, Erikson E, Maller JL (1998) *Science* 282:1701–1704.
25. Cogswell JP, Brown CE, Bisi JE, Neill SD (2000) *Cell Growth Differ* 11:615–623.
26. Hansen DV, Loktev AV, Ban KH, Jackson PK (2004) *Mol Biol Cell* 15:5623–5634.
27. Moshe Y, Boulaire J, Pagano M, Hershko A (2004) *Proc Natl Acad Sci USA* 101:7937–7942.
28. Pines J (2006) *Trends Cell Biol* 16:55–63.
29. Barr FA, Sillje HH, Nigg EA (2004) *Nat Rev Mol Cell Biol* 5:429–440.
30. Vagnarelli P, Earnshaw WC (2004) *Chromosoma* 113:211–222.
31. Riehemann K, Sorg C (1993) *Trends Biochem Sci* 18:82–83.
32. Mundt KE, Golsteyn RM, Lane HA, Nigg EA (1997) *Biochem Biophys Res Commun* 239:377–385.
33. Yamasaki L, Pagano M (2004) *Curr Opin Cell Biol* 16:623–628.
34. Sun L, Chen ZJ (2004) *Curr Opin Cell Biol* 16:119–126.
35. Vong QP, Cao K, Li HY, Iglesias PA, Zheng Y (2005) *Science* 310:1499–1504.
36. Kumagai A, Dunphy WG (1996) *Science* 273:1377–1380.
37. Yoshida H, Jono H, Kai H, Li JD (2005) *J Biol Chem* 280:41111–41121.